Online Supplementary Appendix

Design and Methods

Cell culture. Cell lines were cultured as described in the DSMZ (Human and Animal Cell Lines Database, Braunschweig, Germany) datasheets. Synchronization in S-phase by thymidine and spindle disruption by nocodazole were performed as previously described (1). To test sensitivity to lower concentrations of nocodazole, we performed dilution series (using concentrations of 10, 15, 20, 25 and 30ng/ml nocodazole). For proteasome inhibition, cells were presynchronized in S-phase and MG132 was added in late G2 phase. Induction of expression and knockdown by addition of doxycycline was performed as previously described (2). For selection Kasumi-1, HL-60 and DG-75 cells were grown in the presence of 2.4mg/ml Geneticin and/or 2µg/ml Puromycin and/or 5/10µg/ml Blasticidin. Primary blasts from AML patients were isolated by Ficoll gradient centrifugation from human bone marrow (BM) or peripheral blood (PB). Since primary blasts are almost completely arrested in G1/G0, they were stimulated by cytokines to enter the cell cycle: $2x10^5$ cells per mL were grown in RPMI medium supplemented with 20% FCS, 100ng/ml SCF, 50ng/ml Flt3, 40ng/ml TPO, 50ng/ml IL-3, 20ng/ml IL-6 and 100ng/ml G-CSF (3, 4). The cells were incubated for 96h and then analyzed for BubR1 expression in G2/M by flow cytometry. While cytokine-stimulation works for myeloblastic samples it does not reliably induce growth of lymphoblastic leukemia (personal communication Malcolm Moore, MSKCC (4, 5)). The analyses were carried out according to the guidelines of the Declaration of Helsinki and good clinical practice after informed consent.

Analysis of metaphase chromosomes. Nocodazole-blocked cells were incubated in 0.5% KCl, fixed in methanol (75%v/v)/glacial acetic acid (25%v/v), applied to frozen microscope slides and stained using Giemsa stain (Mallinckrodt). Proper metaphase appearance is defined by the connection of the two sister chromatids. Metaphase spreads displaying single chromatids in the presence of 200ng/ml nocodazole were counted as premature sister chromatid separation events.

Western blot and antibodies. Western blot analyses were performed as previously described (6) using anti-securin (Zymed Laboratories), anti-Bub1 (Dunn Labortechnik), anti-Bub3 (BD Bioscience), anti-Mad2 (Santa Cruz Biotechnology), anti-cyclin B1 (Santa Cruz Biotechnology), anti-Actin (Sigma-Aldrich), anti-alpha-Tubulin (Sigma-Aldrich), anti-BubR1 (BD Biosciences) as primary antibodies. Horseradish-peroxidase-conjugated secondary

antibodies used were anti-rabbit (Amersham Biosciences), anti-mouse (Sigma-Aldrich), anti-goat (Santa Cruz Biotechnology). Densitometric quantification was performed using ImageJ.

In vitro ubiquitination

The APC/C was immunopurified from DG-75 and Kasumi-1 cells using an anti-Cdc27 antibody (Sigma-Aldrich) and Protein G-agarose. Ubiquitination reactions were performed in 40mM Tris pH7.6, 0.5mM DTT, 5mM MgCl, 1mM ATP, 1.5µM ubiquitin aldehyde, 200nM okadaic acid, 125nM UBE1 (Boston Biochem), 1µM UbcH10 (Boston Biochem). Cyclin B was in vitro transcribed/translated (TNT Quick Coupled Transcription/Translation Kit, Promega) in the presence of 35S-marked methionine and used as a substrate.

Flow cytometry. Cells were analyzed by flow cytometry using FACS Calibur (Becton Dickinson). To determine cell cycle-dependent DNA content, cells were fixed in 75% ethanol in PBS for at least 2h at 4°C. DNA was stained using propidium iodide (PI) at a concentration of 5µg/ml, 0.1% Triton X100 and RNase in PBS and incubated for 30min at 37°C. BubR1 shows an increase in protein levels during S- and G2-phase and exhibits maximum concentrations during mitosis (7). To determine BubR1 expression levels per cell in the G2/M phase of cell lines and primary cells by flow cytometry, cells were double-stained with PI, to identify cells with a replicated amount of DNA, and the anti-BubR1 antibody. The protocol used was adapted from the staining procedure for flow cytometric detection of human cyclin which is available at the BD Biosciences homepage. Antibodies used were BubR1 (BD Biosciences), FITC-conjugated goat anti-mouse antibody (DakoCytomation). MOPC-21 (Sigma-Aldrich) was used as an IgG control. BubR1 expression was quantified using the gating strategy described in Suppl. Fig. S1.

Microarray data and data processing. Microarray datasets were obtained from the open-access NIH Gene-Expression Omnibus (GEO) database. Datasets used in our analysis were GSE30029 (8) and GSE13204 (9). For GSE13204, CEL files were downloaded that represent the following clinical subgroups: healthy bone marrow (n=73) and bone marrow from mature B-ALL t(8:14) (n=13), AML t(8;21) (n=40) , AML t(15;17) (n=37), AML 11q23 (n=38), AML inv16 (n=28), AML complex karyotype (n=48), AML normal karyotype (n=351). Using Genedata Expressionist Refiner Array software (Version 7), the CEL files were quantile normalized and condensed using the Robust Multi-array Average (RMA) algorithm. Further data analysis was done with the Analyst module of Expressionist (Version 7). For the calculation of the mean fold change we did not distinguish between clinical subgroups and compared all AML samples against the healthy bone marrow as control. For data set

GSE30029, the preprocessed data as available from GEO were imported into Analyst. Mean expression values for both groups were calculated.

Retroviral transduction. For retroviral transduction, Phoenix alpha packaging cells were transfected with the plasmid of interest and the transduction was performed as previously described (1). For retroviral delivery of fluorescent reporters, a H2-RFP reporter sequence was PCR-amplified from pIRESpuro2b_pH2B-mRFP (kind gift from D. Gerlich, Zurich) and inserted into retroviral backbones (pMX (Cell Biolabs Inc.), pMSCVpuro, pLNCX2 and pLPCX (Clontech)). pLPCX-H2-GFP was a kind gift from S. Taylor. Efficient BubR1 knockdown has been established as described in Suppl. Fig. S2. The oligonucleotide GAAGAGACGATGCCTACAA was used for inducible BubR1 knockdown (two different sequences targeting BubR1 led to compareable results and caused destabilization of cyclin B), modified to fit into RNAi-Ready pSIREN-RetroQ-TetP (Clontech). For retrovirus-delivered inducible expression, the BubR1 and cyclin B coding sequences were PCR-amplified from Hacat cDNA or from a sequence-verified template plasmid and inserted into pRetroX-Tight-Pur (Clontech). Inducible cell lines were established according to the manufacturer's instructions. Experiments with different cell lines expressing H2-RFP, H2-mCherry or without fluorochrome-tagged reporter proteins gave comparable results.

Live-Cell Imaging Kinetics. Cells were seeded on 8-well microscope chambers (Ibidi) that were coated with fibrinogen or collagen IV, at a concentration of 30,000 and 60,000 cells per well and imaged as previously described (1).

Data analysis and statistical analysis. TIFF image stacks were analyzed using LSM Image Browser (v.2.80.1123) (Carl Zeiss). Calculations and statistics were done in Microsoft Excel 2002 and/or GraphPad Prism V5.03 (GraphPad Software Inc.). Statistical significance was considered at p-values <0.05. The statistical test used was an unpaired t-test (two-tailed) with a confidence interval of 95%.

1. Schnerch D, Follo M, Krohs J, Felthaus J, Engelhardt M, Wäsch R. Monitoring APC/C activity in the presence of chromosomal misalignment in unperturbed cell populations. Cell Cycle. 2012 Jan 15;11(2):310-21.

2. Baumgarten AJ, Felthaus J, Wäsch R. Strong inducible knockdown of APC/CCdc20 does not cause mitotic arrest in human somatic cells. Cell Cycle. 2009 Feb 15;8(4):643-6.

3. Engelhardt M, Albanell J, Drullinsky P, Han W, Guillem J, Scher HI, et al. Relative contribution of normal and neoplastic cells determines telomerase activity and telomere length in primary cancers of the prostate, colon, and sarcoma. Clin Cancer Res. 1997 Oct;3(10):1849-57.

4. Engelhardt M, Mackenzie K, Drullinsky P, Silver RT, Moore MA. Telomerase activity and telomere length in acute and chronic leukemia, pre- and post-ex vivo culture. Cancer Res. 2000 Feb 1;60(3):610-7.

5. Engelhardt M, Ozkaynak MF, Drullinsky P, Sandoval C, Tugal O, Jayabose S, et al. Telomerase activity and telomere length in pediatric patients with malignancies undergoing chemotherapy. Leukemia. 1998 Jan;12(1):13-24.

6. Engelbert D, Schnerch D, Baumgarten A, Wäsch R. The ubiquitin ligase APC(Cdh1) is required to maintain genome integrity in primary human cells. Oncogene. 2008 Feb 7;27(7):907-17.

7. Taylor SS, Hussein D, Wang Y, Elderkin S, Morrow CJ. Kinetochore localisation and phosphorylation of the mitotic checkpoint components Bub1 and BubR1 are differentially regulated by spindle events in human cells. J Cell Sci. 2001 Dec;114(Pt 24):4385-95.

8. de Jonge HJ, Woolthuis CM, Vos AZ, Mulder A, van den Berg E, Kluin PM, et al. Gene expression profiling in the leukemic stem cell-enriched CD34+ fraction identifies target genes that predict prognosis in normal karyotype AML. Leukemia. 2011 Dec;25(12):1825-33.

9. Haferlach T, Kohlmann A, Wieczorek L, Basso G, Kronnie GT, Bene MC, et al. Clinical utility of microarray-based gene expression profiling in the diagnosis and subclassification of leukemia: report from the International Microarray Innovations in Leukemia Study Group. J Clin Oncol. 2010 May 20;28(15):2529-37.

Table S1. Patient samples

Patient #	Morphology according to the FAB classification	Source	Percentage of blasts	Cytogenetics
1	AML NOS	BM	84%	trisomy 8
2	sAML from MDS	BM	99%	complex karyotype
3	AML M4eo	BM	99%	inv16 trisomy 22
4	AML NOS	BM	62%	complex karyotype
5	AML M2	BM	92%	t(8;21) monosomy Y
6	AML NOS	BM	99%	trisomy 8 monosomy Y
7	AML NOS	BM	89%	t(3;14)
8	AML M4eo	BM	99%	inv16
9	AML M4eo	BM	99%	inv16
10	AML M1/2	PB	99%	trisomy 11
11	AML M4/5	BM	87%	normal karyotype
12	AML M5b	BM	55%	normal karyotype
13	AML NOS	BM	99%	normal karyotype
14	AML NOS	BM	95%	normal karyotype
15	AML M4eo	BM	90%	inv16
16	AML M3v	BM	80%	t(15;17)
17	AML M5	BM	99%	deletion 9q
18	AML M5a	PB	80%	normal karyotype
19	AML M3v	BM	90%	t(15;17)
20	AML NOS	PB	80%	t(6;9)
21	AML M5a	BM	90%	normal karyotype
22	AML M2	PB	40%	t(8;21)
23	AML M4eo	PB	45%	inv16
24	AML M1	PB	97%	not available
25	AML M3v	PB	88%	t(15;17)
26	AML M1	PB	86%	complex karyotype
27	AML M4eo	BM	70%	inv16
28	AML M5	PB	95%	t(11;19)
29	AML M2	BM	85%	normal karyotype
30	sAML from MDS	BM	55%	normal karyotype
31	relapsed AML NOS	BM	99%	normal karyotype
32	AML M4/5	PB	90%	normal karyotype deletion 20q
33	AML M1	PB	92%	normal karyotype
34	tAML w eosinophilia	BM	65%	monosomy Y
35	AML M1	PB	60%	normal karyotype
36	AML M4/5	BM	75%	normal karyotype
37	AML/SM-AHNMD	PB	n.a.	normal karyotype
38	AML M3v	BM	99%	t(15;17)

NOS = not otherwise specified, s = secondary, PV = polycythemia vera, w = with, BM = bone marrow, PB = peripheral blood, n.a. = not available

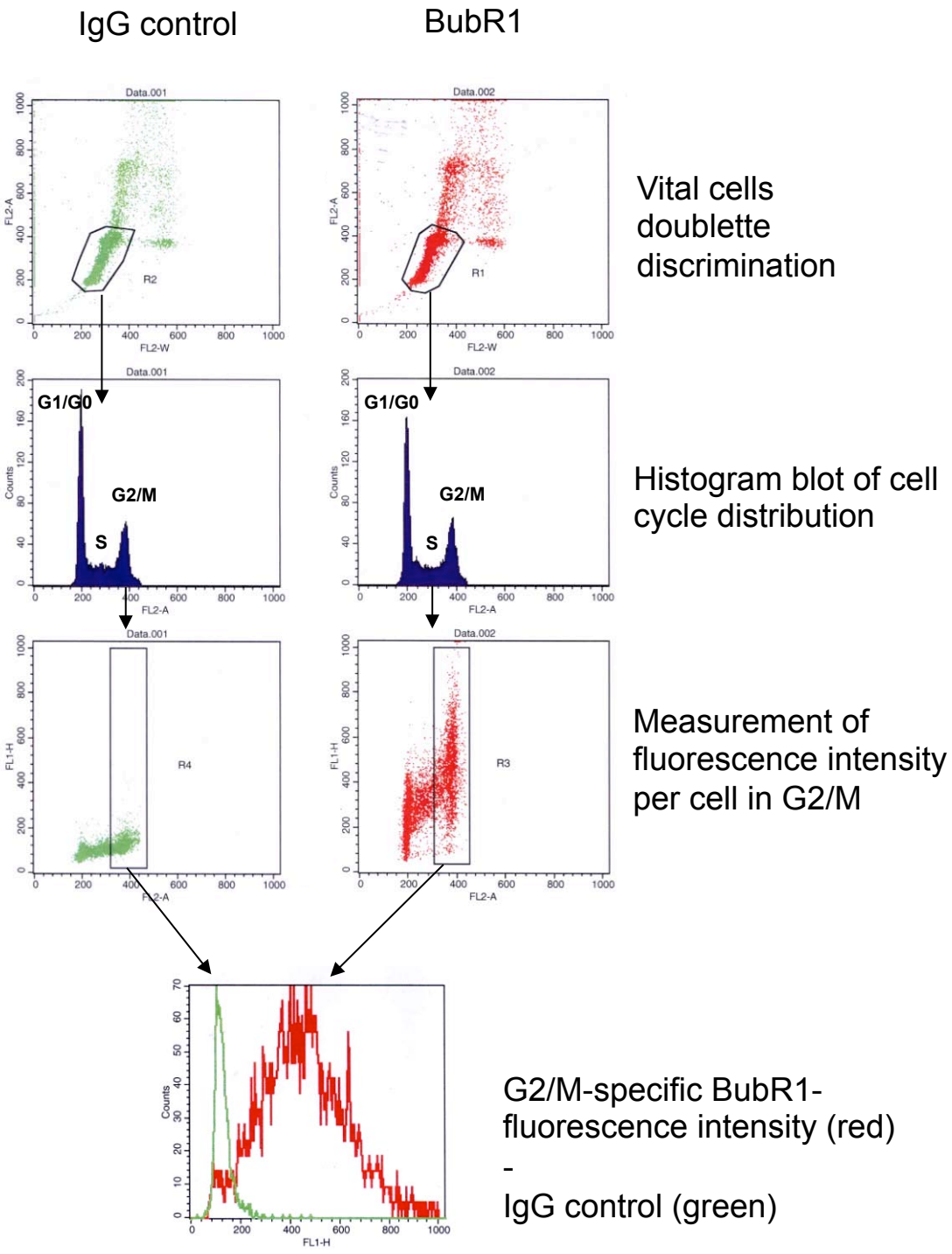

Figure S1. **Dual color flow cytometry allows the selective quantification of BubR1 protein expression in G2/M cells**

Gating strategy for quantification of BubR1 expression in G2/M cells. Following gating of the vital cells, doublets were excluded from the analysis and G2/M cells were selected on the dot plot. Distributions of BubR1 fluorescence intensities were depicted on histogram plots and the mean fluorescence intensity per cell of BubR1- and IgG-control cells was calculated.

Schnerch et al. Figure S1

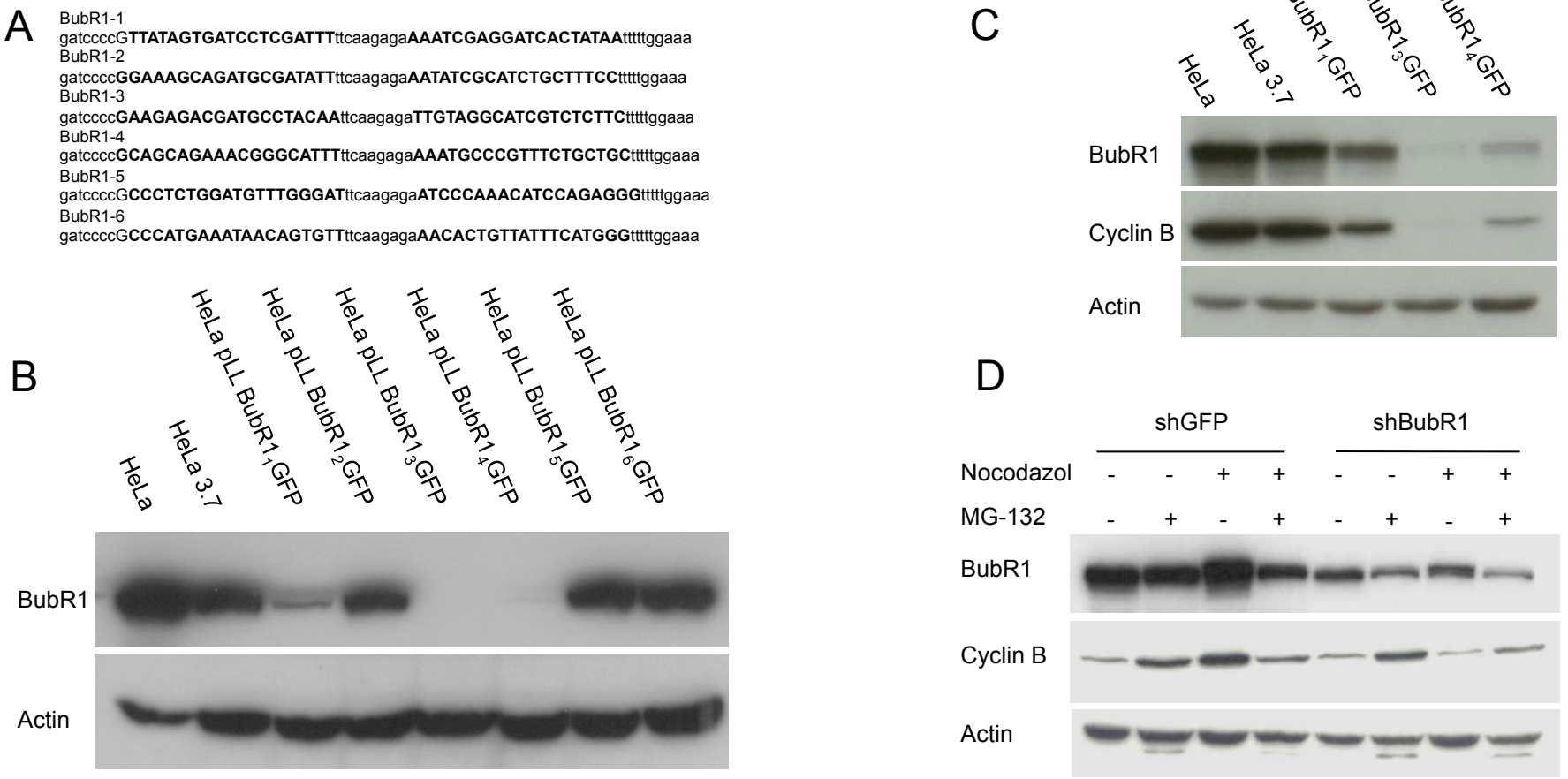

Figure S2. **Establishment of a system allowing a lentivirus-delivered stable knockdown of BubR1**
(A) A set of six different shRNA oligonucleotides were designed to silence BubR1. The top strand for each oligonucleotide pair tested is shown. (B) The oligonucleotides were cloned into pLL3.7 as described elsewhere (Engelbert et al. The ubiquitin ligase APC(Cdh1) is required to maintain genome integrity in primary human cells. *Oncogene* 2008; **27**:907-917). For evaluation of the knockdown effect HeLa cells were subject to lentiviral transduction and transduction efficiencies were assessed by measuring the percentage of GFP-positive cells. (C) In line with recent evidence (Bohers et al. Gradual reduction of BUBR1 protein levels results in premature sister-chromatid separation then in aneuploidy. *Human Genet* 2008; **124**:473-478) we found the strength of the BubR1 knockdown to be associated with downregulation of cyclin B expression levels. (D) To further validate our BubR1 sequences at several different conditions, the knockdown cassettes were cloned into a pLL backbone that expressed the Puromycin resistance gene instead of the GFP gene to allow for longterm selection of transduced cells. As a negative control we included cells that were transduced with a pLL construct specifically targeting GFP. Using these controls, we provided evidence that our knockdown constructs lead to effects as expected from the available data for BubR1 knockdown in the literature.

Schnerch et al. Figure S2

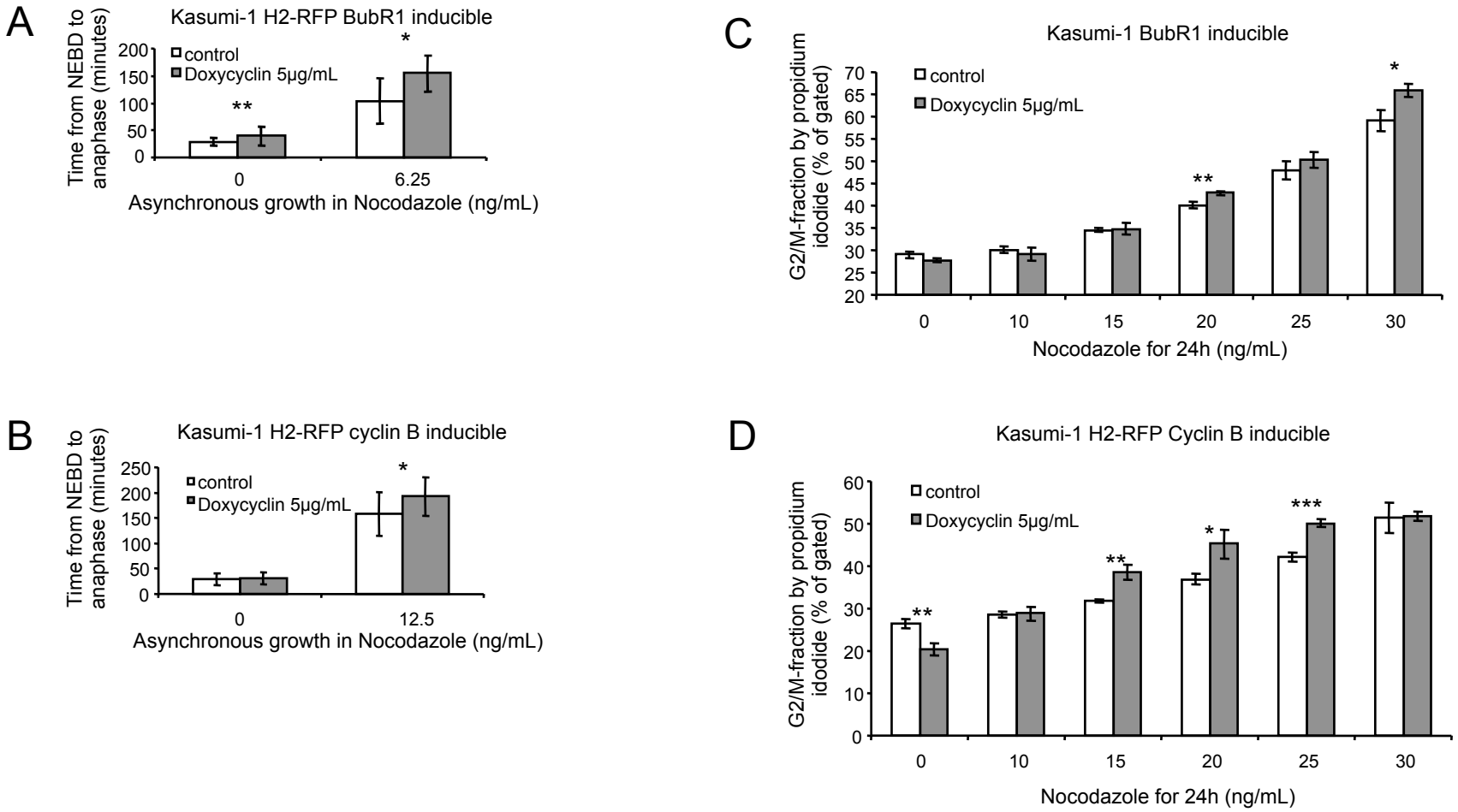

Figure S3. **Accumulation in G2/M and mitotic timing depends on expression levels of BubR1 and cyclin B**
(A) Mitotic timing (nuclear envelope breakdown until anaphase onset) was determined by live-cell imaging of Kasumi-1 cells stably expressing histone H2 fused to the fluorescent marker GFP (H2-GFP). Induction of BubR1 expression was associated with a delayed passage through mitosis both in unperturbed cells and in cells growing in low-dose nocodazole. (B) Induction of cyclin B expression was associated with a delayed passage through mitosis in cells growing in low-dose nocodazole. (c) Quantifications for an ascending series of nocodazole concentrations are shown for BubR1-induced and uninduced Kasumi-1 cells. (D) Quantifications for an ascending series of nocodazole concentrations are shown for cyclin B-induced and uninduced Kasumi-1 cells. *P<.05, **P<.001, ***P<.0001.

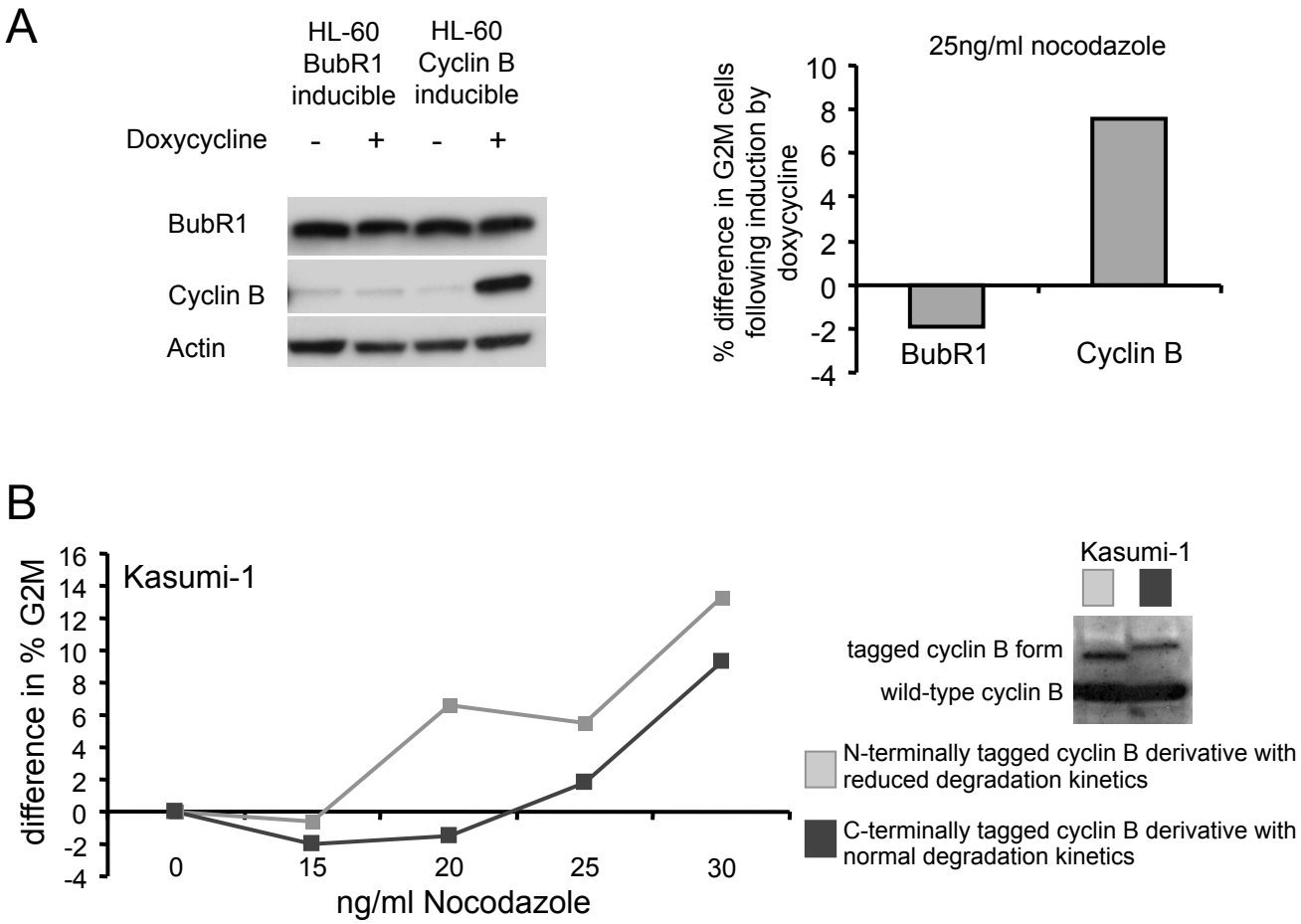

Figure S4. **AML cell lines can be re-sensitized through stabilization of cyclin B**
(A) Inducible expression of BubR1 and cyclin B was established in HL-60, an AML cell line exhibiting higher/normal BubR1 expression levels. The extent to which HL-60 could be re-sensitized to antimitotic treatment upon induction of BubR1 or cyclin B was assessed by flow cytometry in the presence of low-dose nocodazole (mean percent difference in G2M of two independent experiments is shown). (B) In order to provide evidence that the sensitization to spindle poison is the consequence of stabilization of cyclin B we expressed both an N-terminally and a C-terminally tagged cyclin B derivative in the AML cell line Kasumi-1. We reported previously that the N-terminal tag shows reduced degradation kinetics while the C-terminal tag exhibits near-endogenous degradation kinetics (Schnerch D et al. Monitoring APC/C activity in the presence of chromosomal misalignment in unperturbed cell populations. *Cell Cycle* 2012; **11:** 310-321). Both cell lines were challenged with ascending doses of nocodazole and the extent to which cell accumulate in G2M (difference in G2M) was assessed by flow cytometry following PI staining.

Schnerch et al. Figure S4

A

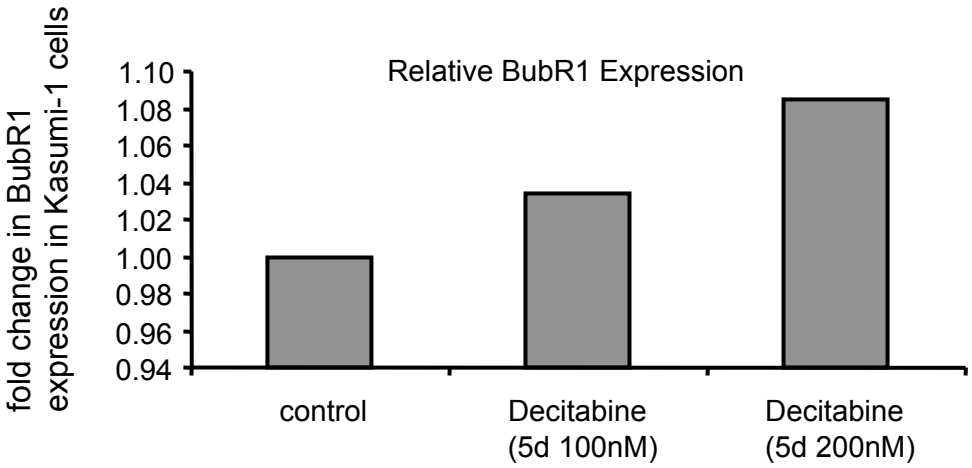

B

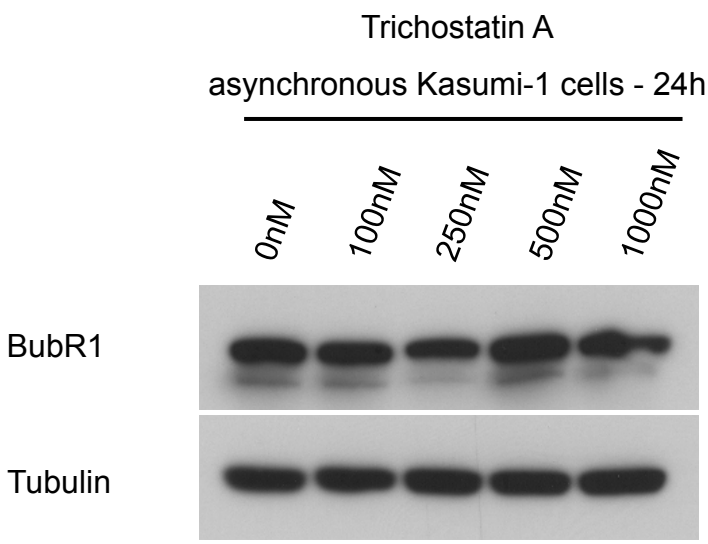

Figure S5. **Mild increase of BubR1 expression levels upon demethylating treatment with decitabine and no change of BubR1 protein levels upon interference with acetylation using trichostatin A**
(A) Since hypermethylation of the BubR1 promotor has been described for a number of malignancies, we tested whether promotor demethylation using decitabine is capable of increasing BubR1 expression. BubR1 expression levels were determined by flow cytometry (Figure S1) and expression levels were normalized to BubR1 expression levels of asynchronously growing Kasumi-1 cells. We detected only a mild increase in BubR1 levels. (B) Since acetylation was recently reported to cause stabilization of BubR1 (Choi et al. BubR1 acetylation at prometaphase is required for modulating APC/C activity and timing of mitosis. *EMBO* 2009; **28**: 2077 – 2089.), we tested whether inhibition of deacetylases by trichostatin A (TSA) at different concentrations increases BubR1 protein levels. We did not observe an effect of TSA on the expression level of BubR1.